Chapter 3
Super-Resolution Microscopy: SIM, STED and Localization Microscopy

James Dodgson, Anatole Chessel, Susan Cox and Rafael E. Carazo Salas

3.1 Introduction

Before looking at the individual super-resolution techniques, it is necessary to briefly introduce or revise a few key concepts that will facilitate understanding them.

The Microscope Is a Low-Pass Spatial Frequency Filter In very simple terms, a microscope illuminates a sample, collects the light diffracted by the sample with a lens and then builds an interference pattern that is viewed as an image on the back focal plane. Not all the diffracted light is collected by the lens (Fig. 3.1a), and consequently the highest spatial information is lost. A diffraction-limited image is therefore "fuzzy" or "blurred". This is demonstrated in Fig. 3.1b, where the point spread function (PSF) of a single point source of light (a single fluorescent bead 100 nm in diameter) is shown. In "conventional" or "diffraction-limited" microscopy, the PSF will be of a size that depends on the precise optics and on the wavelength of light used. For fluorescence microscopy, this would not generally be smaller than ~200 nm in the lateral plane and ~500 nm in the axial plane. This is the resolution

J. Dodgson (✉) · R. E. Carazo Salas
Genetics Department, University of Cambridge, Downing Street, Cambridge CB2 1EH, UK
e-mail: jd535@cam.ac.uk

R. E. Carazo Salas
e-mail: cre20@cam.ac.uk

A. Chessel
Department of Genetics, University of Cambridge, Tennis Court Road, Cambridge CB2, 1PD, UK
e-mail: ac744@cam.ac.uk

S. Cox
Randall Division of Cell and Molecular Biophysics, King's College London, New Hunt's House, Guy's Campus, London SE1 1UL, UK
e-mail: susan.cox@kcl.ac.uk

T. E. S. Dahms and K. J. Czymmek (eds.), *Advanced Microscopy in Mycology,* Fungal Biology, DOI 10.1007/978-3-319-22437-4_3

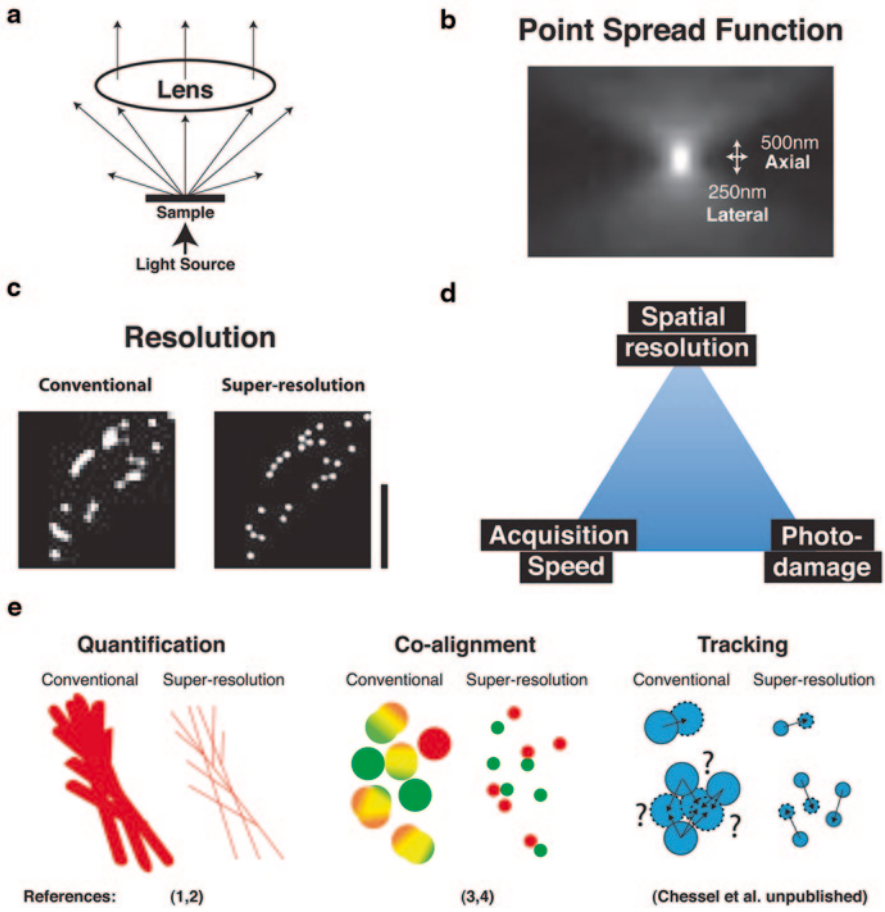

Fig. 3.1 Basic concepts. **a** The lens fails to collect all the diffracted light from a sample being illuminated, and as a consequence high-resolution spatial information is lost. **b** The point spread function of a 100-nm-diameter fluorescent glass bead is 250 nm laterally and 500 nm axially. **c** Conventional imaging cannot allow many of the proximal glass beads to be distinguished, but super-resolution imaging can. **d** The super-resolution imaging-limitation triangle (as formulated by and with kind permission from Eric Betzig). **e** Graphical representation of the some of the potential insights that super-resolution microscopy has to provide to fungal cell imaging. Scale bar is 2 μm

limit, and it restricts the potential of imaging to resolve (or distinguish between) two points that are close together (Fig. 3.1c).

Super-Resolution Super-resolution breaks the diffraction limit, allowing the differentiation of conventionally unresolvable objects (see Fig. 3.1c). This relatively recent development is reviewed in the context of three main super-resolution techniques currently available. When evaluating the relative merits of each technique, we need to consider the limitations of spatial resolution (both lateral and axial),

photodamage (a combination of photobleaching and phototoxicity) and acquisition speed. Improvements in any one factor are usually to the detriment of the other two, expressed in the form of "the super-resolution imaging-limitation triangle" (Fig. 3.1d). These limitations are especially crucial in the realm of live-cell imaging. Thus the first, and maybe most important, part of any super-resolution experiment is to choose the most appropriate technique.

In the following sections, we give a primer of three super-resolution imaging techniques as applied to mycological research. As the field of super-resolution microscopy is one that is wide and rapidly evolving, rather than doing a comprehensive review, we stay within the confines of the more mainstream techniques that have been commercialized and demonstrated to be useful for work in fungi.

The Value of Super-Resolution Imaging The value of these techniques to fungal cell biology is demonstrated by the citation of specific examples in fungal live- and fixed-cell imaging. Figure panel 3.1e provides a graphical summary of some of the potential insights that super-resolution imaging can unlock, including the accurate quantification of structures including their number and size (Miao et al. 2013; Puchner et al. 2013), an accurate assessment of co-alignment and other spatial arrangements between structures (Daboussi et al. 2012; Voelkel-Meiman et al. 2013) and allowing the tracking of dynamic structures otherwise too densely packed to distinguish (Chessel et al. Unpublished). This is by no means a comprehensive list, and many other applications are and will be possible for techniques that reveal the cell in such high levels of detail.

3.2 Structured Illumination Microscopy

Structured illumination microscopy (SIM) imaging approximately doubles the resolution both axially and laterally compared with conventional wide-field microscopy (Gustafsson 2000). For a typical fluorophore, it can resolve features separated by 110–130 nm in the lateral plane and 250 nm in the axial plane. A strong attribute is that 3D image acquisition is a routine and usually constitutive component of the SIM imaging process. SIM is also relatively easy to use, can be used on multiple standard fluorophores with no special sample preparation, and the newest platforms can do all this using live cells. For imaging of structures whose physical size lies in that range, SIM is possibly the most enticing super-resolution platform.

The principles underlying SIM are summarized very briefly in Fig. 3.2a. It involves the acquisition of several images of the same sample using light modulated by a periodic pattern of various orientations. The interference between the periodic pattern and the structure of the sample creates a Moiré pattern. This interference pattern contains downshifted high-frequency information. An algorithm is then used to reconstruct a single super-resolved image. For a far more detailed outline of the principles of structured illumination, the paper by Schermelleh (Schermelleh et al. 2008) is recommended.

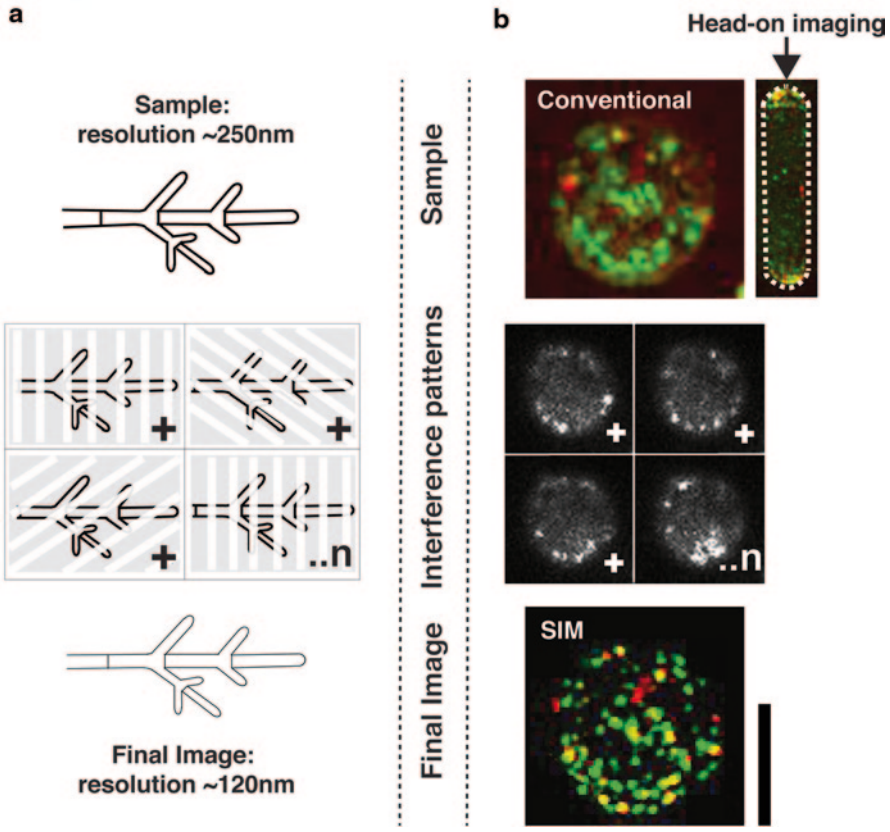

Fig. 3.2 Structured illumination microscopy (SIM) microscopy. **a** Principles underlying SIM microscopy. High spatial frequencies normally not assessable are collected by illuminating the sample with interference patterns created through a gridding pattern. Individual images are captured as the gridding device is shifted and rotated. The images are then processed by a computer algorithm to generate a super-resolved image. **b** Live-cell SIM versus conventional deconvolved wide-field images with an OMX BLAZE microscope (applied precision). Imaging Tea1-3mCherry (Tea1-3mCh, *red*) and Tea3-Green Fluorescent Protein (Tea3-GFP, *green*) polarity factors in the cell end of the fission yeast. Side-on cell was taken by conventional microscopy. Both head-on panels are maximum intensity projections of 2-µm-deep image z-stacks in the same cell (Chessel et al. Unpublished). The polarity factor clusters are resolvable to around 120 nm in size. Scale bar is 2 µm

A requirement of SIM is the acquisition of multiple "raw" images, which are then consequently processed to generate a single super-resolved image or stack. For this reason, acquiring a large number of "raw" images can limit SIM's applicability to live-cell microscopy mainly due to the effects of poor temporal resolution and potentially high photodamage. Newer commercial platforms are now available with very rapid image acquisition and are marketed for live-cell imaging. These still may not be suitable for very dynamic structures, whilst the very short exposure times

required may not offer sufficient sensitivity for weak signals. SIM in most systems is a wide-field technique, and consequently acquiring good-quality images within thick specimens, where the object plane is a distance away from the coverslip, may be difficult (a limit of 10-μm distance from the coverslip is typical in one commercial system). Recently SIM has been combined with ultrathin planar illumination, which improves imaging within thick specimens and reduces the effects of high photodamage (Gao et al. 2012).

3.2.1 Applications in Mycological Imaging

Fixed Cell

SIM's relative ease of applicability extends to its compatibility with standard fixation and labelling methods found in conventional yeast microscopy. Structures that appear to be punctated by conventional microscopy can often be resolved into multiple different structures by super-resolution imaging. For example, 3D-SIM has been used to more accurately describe and quantitate densely arranged structures in yeast cells, such as linear actin cables stained with phalloidin in *Saccharomyces cerevisiae* (budding yeast) cells (Miao et al. 2013) and punctate polarity factors observed in *Schizosaccharomyces pombe* (fission yeast) cell ends labelled with a standard secondary antibody (Dodgson et al. 2013). Multicolour super-resolution microscopy can also allow a more exact determination of the nature of correlation between proteins or cellular structures. Even structures that appear to closely co-localize may no longer do so following a reduction in their PSFs by SIM. For example in budding-yeast vesicle assembly Gga2p-RFP (Red Fluorescent Protein) and β1-GFP, puncta overlap in conventional confocal imaging but are usually adjacent and distinct with 3D-SIM imaging (Daboussi et al. 2012). Also in budding yeast, more precise two-colour imaging has revealed at the organelle level that mitochondria are not associated with the endoplasmic reticulum (Swayne et al. 2011). Even between structures or proteins which still co-align with two-colour SIM, a reduction in their PSF size can now allow precise mapping of their respective spatial positions. For example, the protein SUMO was sufficiently resolved by 3D-SIM that it could now be positioned centrally within the budding-yeast synaptonemal complex (Voelkel-Meiman et al. 2013). Similarly, 3D-SIM was applied to precisely map the spatial layout of components of the replication factory with respect to their deoxyribonucleic acid (DNA) template (Saner et al. 2013).

Live Cell

Combining 2D-SIM with total internal reflection fluorescence (TIRF) microscopy can improve the compatibility of SIM with live-cell imaging (Dobbie et al. 2011). This has been used to image cortical proteins in live budding-yeast cells (Spira et al.

2012). As previously mentioned, the newest commercial systems have faster acquisition times and can realistically achieve live-cell 3D-SIM (lapses every ~1.2 s for a 2-μm-thick stack are possible in a commercial system). Commonly used tags such as GFP and mCherry are suitable, although they will be susceptible to photobleaching during the raw image acquisition. Figure 3.2b from our own work demonstrates live-cell 3D-SIM of labelled polarity factor clusters in a fission yeast cell end. The same polarity factor clusters can also be viewed by time-lapse imaging at 1-s intervals for around ten time points allowing the first direct tracking of these dynamic structures (Chessel Unpublished). Live-cell 3D-SIM has also been applied to map the proximity of mis-folded proteins to the budding-yeast vacuole membrane (Spokoini et al. 2012).

3.2.2 SIM Summary

SIM is arguably the least difficult super-resolution technique to apply, requiring little if any extra sample preparation compared to conventional microscopy and having, toward the same applicability in terms of 3D, multicolour and now live-cell imaging. Whilst the improvement in resolution is somewhat less than other super-resolution techniques, SIM is often advisable as a starting point before trying more difficult techniques. The achievable resolution might be sufficient for your imaging goals, and if the sample contains too much background to achieve good results, it will quickly become apparent. The extended raw image acquisition should not affect typical fixed-cell imaging (although anti-fade agents are advisable to reduce the effects of photobleaching) but may prove a limitation for live-cell imaging if the signal is weak, where increasing the illumination intensity leads to strong photobleaching and loss of signal. As a point of caution, it must be noted that structured illumination is susceptible to various artefacts resulting from factors including photobleaching, inaccurate system calibration, poor matching of the immersion oil refractive index to the sample leading to inaccurate or hard to interpret algorithmic reconstruction (Schaefer et al. 2004).

3.3 Stimulated Emission Depletion Microscopy

Unlike SIM or localization microscopy (LM), which are usually wide-field microscopy techniques, stimulated emission depletion (STED) microscopy is based on a confocal system (see Chap. 1). It might therefore be especially suited, with certain adaptations, to imaging of mycological samples growing in thick cultures where out of focus or scattered light would impair imaging quality (Gould et al. 2012). In yeast, live-cell STED with fluorescent proteins is now possible with resolution below 60 nm in the lateral plane (Stagge et al. 2013; Rankin et al. 2011).

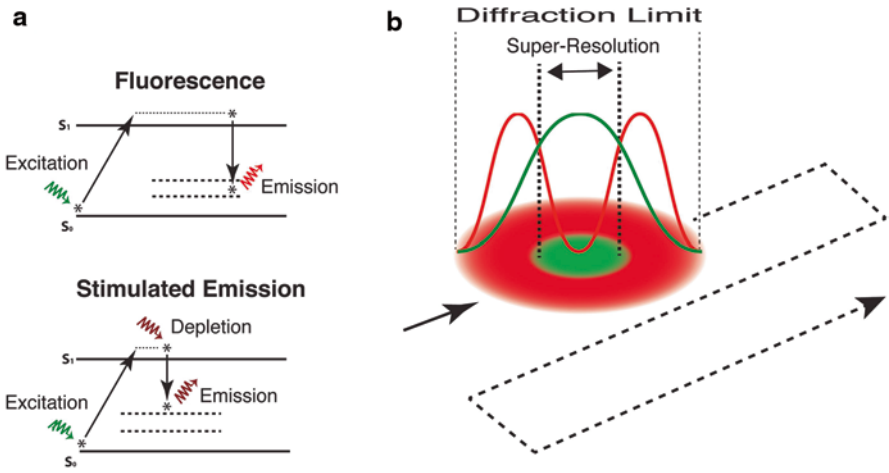

Fig. 3.3 Principles underlying stimulated emission depletion (STED) microscopy. **a** Highly simplified Jablonski diagram illustrating the transitions in electronic state during normal fluorescence and during stimulated emission. In normal fluorescence, a molecule is excited by light of shorter wavelength and then emits light of longer wavelength whilst transitioning back to an unexcited state. Stimulated emission of the excited molecular state by an additional depletion laser causes the emitted light to be of sufficiently longer wavelength and shorter fluorescent lifetime so that it can consequently be separated from normal fluorescence. **b** A doughnut-shaped depletion laser (in *red*) effectively reduces the point spread function (PSF) of normal fluorescence (in *green* and marked by a *double arrow*) below its diffraction limit since only the unstimulated light from the centre of the doughnut is collected. The sample is scanned with this arrangement as for conventional scanning confocal microscopy

STED is also different from SIM or LM in that generation of the super-resolved image is not finalized by a mathematical reconstruction but rather depends on a physical suppression of the effective PSF size (although deconvolution can be applied to improve image quality). This is summarized in Fig. 3.3 from an excellent review by Muller et al. 2012 which is also recommended for a much more in-depth description of the principles and methodology surrounding STED imaging. In brief, a diffraction-limited excitation spot is projected onto the sample together with a doughnut-shaped depletion beam that will restrict normal fluorescence to a central area smaller than the diffraction limit (Müller et al. 2012). Increasing the power of the depletion beam will increase the area of fluorophore depletion and further reduce the effective PSF. The depletion beam however also enhances photodamage and so is associated with signal loss that together can make STED imaging of weak signals difficult. It is also important to note that in conventional STED there is no impact on PSF in the axial plane, and consequently resolution is not improved along the *z*-axis (Farahani et al. 2010), although further implementations have been developed to partially rectify this (Laporte et al. 2013).

Table 3.1 Generalized relative attributes of the super-resolution techniques

System	Lateral Resolution	Axial Resolution	Platform	3D	Speed	Labels
SIM	~120nm	~250nm	Widefield	Routine	••	Standard fluorophores
STED	~60nm	No Gain	Confocal	Non-Routine	••• (Dependent on frame size)	Standard fluorophores
LM	~20nm	~20nm	Widefield	Non-Routine	•	Photoswitchable fluorophores

3.3.1 Applications in Mycological Imaging

Fixed Cell

STED has been mainly applied to immunofluorescently labelled fixed samples, and special fluorophores are usually required for STED. There are a range of commercially available dyes suitable for STED conjugated to secondary antibodies and with varied spectral properties (Table 3.1 of the review by Muller et al. 2012 recommends as a list of potential dyes). It should be noted that multicolour resolution most commonly requires two dyes which can be both depleted with the same laser.

Live Cell

Exploration of STED as a live-cell imaging technique has frequently used yeast as the imaging sample in proof-of-principle demonstrations. In the proof-of-principle application of STED to live cells, the vacuole membrane of *S. cerevisiae* cells was stained with the dye RH-414 (Klar et al. 2000). Staining with dyes as a method of live-cell labelling is very limited in application, but with fluorescently labelled proteins, there is much greater flexibility. For STED imaging in *S. cerevisiae,* this has been achieved by genetically fusing selected proteins with tags that bind to exogenous fluorescent labels (Stagge et al. 2013; Fitzpatrick et al. 2009) and by making use of new laser combinations to image GFP (Rankin et al. 2011). Using either method to image eisosomes at the cortex, lateral resolution below 60 nm was possible (Stagge et al. 2013; Rankin et al. 2011).

3.3.2 Stimulated Emission Depletion Microscopy Summary

Although yeast cells have been used as an exemplar sample in the development of STED, it is not yet widely used in mycology research for elucidating real biological questions. STED has potentially higher resolution than SIM in the lateral plane and

will not generate artefacts from mathematical reconstructions. Fluorophore availability and high photodamage might be more limiting than other techniques, and as this is a confocal-based technique, the frame rate will scale with image size (or higher laser intensities must be used). Three-dimensional imaging is possible only with further techniques not yet commercially available (Wildanger et al. 2009). As suggested, it is possible that (with adjustment of the objective correction to correct for aberrations) STED will be most suitable for imaging of samples that exist in thick cultures (Gould et al. 2012).

3.4 Localization Microscopy

LM includes a group of related techniques such as photoactivated localization microscopy (PALM), fluorescence photoactivation localization microscopy (fPALM, see also Chap. 2), stochastic optical reconstruction microscopy (STORM) and ground state depletion microscopy followed by individual molecule return (GSDIM) based on the same principles outlined in Fig. 3.4a (Rust et al. 2006; Hess et al. 2006; Betzig et al. 2006, Fölling et al. 2008). By analysing the PSF of a single fluorophore, it is possible to determine its position with an accuracy dependent on the number of collected photons and the level of background. In standard experimental conditions, the PSF can then be substituted with a feature ten times smaller than the size of the PSF itself, allowing resolution well below the diffraction limit of the microscope.

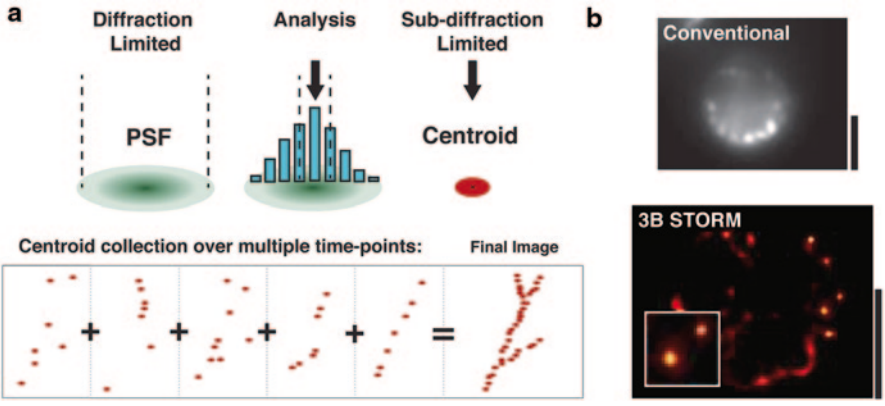

Fig. 3.4 Localization microscopy (LM). **a** Principles underlying LM. The point spread function *(PSF)* of a single fluorophore is diffraction limited in size but can be analysed to determine its centre to within an area below the diffraction limit. If emission is temporally controlled so that individual *PSFs* are distinguishable from each other, then individual points can be collected sequentially to generate a final super-resolved image. **b** Live-cell imaging of the polarity factor Tea3-Green Fluorescent Protein (Tea3-GFP) in the cell ends of fission yeast by conventional imaging and processed with 3B LM (our unpublished data). *Inset area* is double magnification showing individual clusters resolvable to 60 nm in size. Raw images taken on an OMX microscope. Scale bars 2 μm. *STORM* stochastic optical reconstruction microscopy

In biological samples, the PSFs of neighbouring fluorophores will usually overlap extensively rendering them inseparable. In LM, PSF overlap is avoided by temporal separation, with only a small fraction of all the fluorophores activated at any single time point. Over multiple time points (which may total several thousands in a typical LM experiment), a final super-resolved image is generated from the accumulated centroidal points. Activating only a subset of fluorophores in each time point is the key to LM, and the exact methods vary between different techniques. It is essential that both the PSF of the single fluorophore be detectable over the background (with enough photons to give a good localization accuracy) and that it be sufficiently distinct from other fluorophores excited at a given time point. A resolution of around 20 nm is possible in biological samples. Three-dimensional and multicolour imaging are possible, though not necessarily routine. Live-cell LM is difficult for similar reasons as live-cell SIM, in that the large number of individual image acquisitions required can lead to poor time resolution and to photodamage.

3.4.1 Applications in Mycological Imaging

Fixed Cell

In budding yeast, multicolour STORM imaging with photo-switchable dye pairs was used to image "barcoded" messenger ribonucleic acid (mRNA) transcripts (Lubeck and Cai 2012). In conventional microscopy, only low copy transcripts can be labelled because overlapping fluorophores cannot be differentiated. By contrast, STORM only sparsely activates overlapping fluorophores allowing much higher copy-number transcripts to be analysed.

LM with conventional fluorophores is now achievable with direct stochastic optical reconstruction microscopy (dSTORM; van de Linde et al. 2011). This technique was used to measure the size of clusters of the polarity factor Tea1 at fission yeast cell ends, labelled with a secondary antibody conjugated to the fluorophore AF-647 (Dodgson et al. 2013). With consideration given to both localization uncertainty and antibody size, the estimated resolution limit for those experiments of 42.5 nm was below the median Tea1 cluster size measured at around 75 nm, thus providing boundaries for the size of these structures.

Live Cell

Live-cell LM is possible with photo-switchable dyes (described in Chap. 2) or with photo-activatable proteins (Jones et al. 2011). In budding yeast, tagging of a PI3P reporter with mEos2 and live-cell PALM imaging allowed the maturation pattern of vesicles to be followed with multileveled detail (Puchner et al. 2013). With a resolution of 20 nm, vesicles with an average diameter of 80 nm could be accurately distinguished and measured in size. Furthermore, quantitative live-cell PALM was

applied concurrently to molecule counting in the same vesicles. Molecules closely packed together could be individually counted, as during PALM imaging they are temporally separated. Such quantification required *in vivo* calibration methods that correct for over-counting from blinking and undercounting from non-maturation of the fluorophore. The number of molecules per vesicle was found to correlate with vesicle size as expected, and its measure contributed to understanding vesicle progression. A similar methodology was deployed to measure the number of CENP-A^{cnp1} tagged with mEos2 at the fission yeast centromere (Lando et al. 2012). Interestingly, relative deposition of CENP-A^{cnp1} molecules was found to peak in the later stages of the cell cycle. However, lack of agreement with other methods in the absolute counting of CENP-A^{cnp1} led to caution from the authors regarding the accuracy of their method for absolute measurements.

Three-dimensional LM is generally not routine, but by using a multifocal microscope in combination with PALM, Wisniewski et al. 2014 were able to image Cse4-tdEos at the budding-yeast centromere within a depth of ~4 μm and an axial resolution of ~50 nm. Using this approach, the Cse4 centromeric clusters were found to alter their size and shape during the cell cycle from a spherical grouping of ~400 nm in G1 to an ellipse grouping ~350 and ~200 nm in diameter.

Another live-cell LM technique is Bayesian analysis of blinking and bleaching (3B) LM (Cox et al. 2011), which is based on the natural blinking and bleaching properties of some fluorophores (such as GFP). This method creates a hidden Markov model of the dataset, including the blinking and bleaching properties of the fluorophores. This allows information to be extracted from data where many fluorophores are overlapping in each frame. The advantage of this approach is the relative ease by which it can be applied to imaging on standard microscopes with standard fluorophores. From our own 3B LM imaging, dynamic Tea3-GFP clusters at the fission yeast cell end could be tracked at a spatial resolution of 60 nm and a time resolution of 1.4 s (Fig. 3.4b).

In LM, because the final image is generated over multiple time points, there is a requirement for the target cell to be held very still over a prolonged period. Live fission yeast cells were immobilized with a microfluidic device that held and sustained the cells within a flow of media (Bell et al. 2014). Proof-of-principle PALM imaging of the centromere with mEos2-Cnp1 was then performed. The authors suggest that this method provides a more "natural" environment than trapping cells within gels for super-resolution imaging (Bell et al. 2014).

3.4.2 LM Summary

LM is the widest and fastest moving of the branches of super-resolution imaging. The sheer number of different techniques is vast and can seem bewildering. In biological samples, LM can achieve better resolution than SIM and STED, and 3D and multicolour imaging is becoming increasingly common. Live-cell PALM with protein tags like mEos2 is a particularly exciting technique, potentially requiring little sample preparation and extending to molecule counting as well as structure visualization.

3.5 Summary

The resolution limit of the conventional microscope has been a major barrier to the ability of biologists to accurately describe the detailed mechanisms of cells. The advent of super-resolution microscopy has and is increasingly pushing this boundary back in what represents an imaging revolution. Previously indistinguishable structures can be identified, accurately measured and tracked and the spatial relationships between protein pairs more closely described, and now even the quantification of proteins within a structure is possible.

Beginning with the biological question of interest that might be answered by super-resolution imaging, choose a technique that will most directly provide the solution. This review has covered the relative attributes of SIM, STED and LM imaging (generalized in Table 3.1), but in reality the relative performance and applicability of a technique are going to be highly experiment specific and may involve considerations and compromises not featured in this review. SIM is the most straightforward technique to apply, with 3D, multicolour and time-lapse imaging as a routine feature. SIM is not usually suitable for imaging in thick specimens and has less resolution than STED and LM. STED is a confocal-based technique so could be more suitable for imaging far away from the coverslip, and its potential lateral resolution is better than SIM. 3D and multicolour STED imaging are not yet routine, and the frame rate in time-lapse imaging depends on the image size. LM imaging has potentially the best resolution of all the techniques, but 3D and multicolour imaging within thick specimens may be difficult. Be aware that super-resolution fixed- and live-cell imaging represent two very different sized challenges with all three techniques associated with a potential decrease in speed and photostability that might render it difficult with live-cell imaging.

The uptake of super-resolution in the mycological field has arguably been slow, with a similar paper in the bacterial field able to review from a far larger group of experimental papers (Coltharp and Xiao 2012). Any lack of uptake is presumably the result of unfamiliarity with new techniques and maybe more because super-resolution platforms, although commercially available, are still fairly scarce, sometimes expensive and certainly less available than conventional ones. Super-resolution microscopy is a new technology in the early adoption phase, so if as likely you are not in an institution with the suitable instruments for your aims, then be prepared to be proactive in searching for potential hosts and collaborations. It is advisable to establish contacts and gain advice from imaging experts within your own institution and any visiting speakers with experience of super-resolution imaging. Be persistent in approaching the relevant people or groups with access to the relevant systems, and once an understanding is reached, then you will probably have to travel to the site of the super-resolution platform. Your hosts or collaborators are also likely to be experts in this field and a valuable source of advice.

For decades the diffraction limit has stood before the biological investigator as a barrier to be aware of but not to be overcome. The dawn of the super-resolution microscope has now broken this limit and represents an opportunity to describe your biological system with new radical detail.

Acknowledgments We would like to thank Nicola Lawrence and Alex Sossick for assistance with imaging and Eric Betzig for use of the super-resolution imaging-limitation triangle. This work was supported by an European Research Council (ERC) Starting Researcher Investigator Grant (R.E.C.-S., J.D.; SYSGRO), a Human Frontier Science Program (HFSP) Young Investigator Grant (R.E.C.-S., A.C., J.D.; HFSP RGY0066/2009-C), Biotechnology and Biological Sciences Research Council (BBSRC) Responsive Mode grant (R.E.C.-S., A.C., J.D.; BB/K006320/1) and an MRC grant (S.C.). S.C. was also supported by a Royal Society University Research Fellowship.

References

Bell L, Seshia A, Lando D, Laue E, Palayret M, Lee SF, Klenerman D (2014) A microfluidic device for the hydrodynamic immobilisation of living fission yeast cells for super-resolution imaging. Sens Actuators B Chem 192:36–41

Betzig E, Patterson GH, Sougrat R, Lindwasser OW, Olenych S, Bonifacino JS et al (2006) Imaging intracellular fluorescent proteins at nanometer resolution. Science 313(5793):1642–1645

Chessel A, Boussier J, Dodgson J, Carazo-Salas RE (Unpublished) Investigating single particle cortical polarity nanocluster dynamics without tracking

Coltharp C, Xiao J (2012) Superresolution microscopy for microbiology. Cell Microbiol 14(12):1808–1818

Cox S, Rosten E, Monypenny J, Jovanovic-Talisman T, Burnette DT, Lippincott-Schwartz J et al (2011) Bayesian localization microscopy reveals nanoscale podosome dynamics. Nat Methods 9(2):195-200. doi:10.1038/nmeth.1812

Daboussi L, Costaguta G, Payne GS (2012) Phosphoinositide-mediated clathrin adaptor progression at the trans-Golgi network. Nat Cell Biol 14(3):239–248

Dobbie IM, King E, Parton RM, Carlton PM, Sedat JW, Swedlow JR et al (2011) OMX: a new platform for multimodal, multichannel wide-field imaging. Cold Spring Harb Protoc 2011(8):899–909

Dodgson J, Chessel A, Yamamoto M, Vaggi F, Cox S, Rosten E et al (2013) Spatial segregation of polarity factors into distinct cortical clusters is required for cell polarity control. Nat Commun 4:1834–1839 (Nature Publishing Group. 1AD)

Farahani J, Schibler M, Bentolila L (2010) Stimulated emission depletion (STED) microscopy: from theory to practice. Microscopy: Science, Technology, Applications and Education

Fölling J, Bossi M, Bock H, Medda R, Wurm CA, Hein B et al (2008) Fluorescence nanoscopy by ground-state depletion and single-molecule return. Nat Methods 5(11):943–945

Fitzpatrick JAJ, Yan Q, Sieber JJ, Dyba M, Schwarz U, Szent-Gyorgyi C et al (2009) STED nanoscopy in living cells using Fluorogen Activating Proteins. Bioconjug Chem 20(10):1843–1847

Gao L, Shao L, Higgins CD, Poulton JS, Peifer M, Davidson MW et al (2012) Noninvasive imaging beyond the diffraction limit of 3D dynamics in thickly fluorescent specimens. Cell 151(6):1370–1385

Gould TJ, Burke D, Bewersdorf J, Booth MJ (2012) Adaptive optics enables 3D STED microscopy in aberrating specimens. Opt Express 20(19):20998–21009

Gustafsson MG (2000) Surpassing the lateral resolution limit by a factor of two using structured illumination microscopy. J Microsc 198(Pt 2):82–87

Hess ST, Girirajan TPK, Mason MD (2006) Ultra-high resolution imaging by fluorescence photoactivation localization microscopy. Biophys J 91(11):4258–4272

Jones SA, Shim S-H, He J, Zhuang X (2011) Fast, three-dimensional super-resolution imaging of live cells. Nat Methods 8(6):499–508

Klar TA, Jakobs S, Dyba M, Egner A, Hell SW (2000) Fluorescence microscopy with diffraction resolution barrier broken by stimulated emission. Proc Natl Acad Sci U S A 97(15):8206–8210

Lando D, Endesfelder U, Berger H, Subramanian L, Dunne PD, McColl J et al (2012) Quantitative single-molecule microscopy reveals that CENP-A(Cnp1) deposition occurs during G2 in fission yeast. Open Biol 2(7):120078

Laporte GPJ, Conkey DB, Vasdekis A, Piestun R, Psaltis D (2013) Double-helix enhanced axial localization in STED nanoscopy. Opt Express 21(25):30984

Lubeck E, Cai L (2012) Single-cell systems biology by super-resolution imaging and combinatorial labeling. Nat Methods 9(7):743–748

Miao Y, Wong CCL, Mennella V, Michelot A, Agard DA, Holt LJ et al (2013) Cell-cycle regulation of formin-mediated actin cable assembly. Proc Natl Acad Sci U S A 110(47):E4446–E4455

Müller T, Schumann C, Kraegeloh A (2012) STED microscopy and its applications: new insights into cellular processes on the nanoscale. Chemphyschem 13(8):1986–2000

Puchner EM, Walter JM, Kasper R, Huang B, Lim WA (2013) Counting molecules in single organelles with superresolution microscopy allows tracking of the endosome maturation trajectory. Proc Natl Acad Sci U S A 110(40):16015–16020

Rankin BR, Moneron G, Wurm CA, Nelson JC, Walter A, Schwarzer D et al (2011 Jun 22) Nanoscopy in a living multicellular organism expressing GFP. Biophys J 100(12):L63–L65

Rust MJ, Bates M, Zhuang X (2006) Sub-diffraction-limit imaging by stochastic optical reconstruction microscopy (STORM). Nat Methods 3(10):793–795

Saner N, Karschau J, Natsume T, Gierlinski M, Retkute R, Hawkins M, et al (2013) Stochastic association of neighboring replicons creates replication factories in budding yeast. J Cell Biol 202(7):1001–1012

Schaefer LH, Schuster D, Schaffer J (2004) Structured illumination microscopy: artefact analysis and reduction utilizing a parameter optimization approach. J Microsc 216(Pt 2):165–174

Schermelleh L, Carlton PM, Haase S, Shao L, Winoto L, Kner P et al (2008 Jun 6) Subdiffraction multicolor imaging of the nuclear periphery with 3D structured illumination microscopy. Science 320(5881):1332–1336

Spira F, Mueller NS, Beck G, Olshausen von P, Beig J, Wedlich-Soldner R (2012) Patchwork organization of the yeast plasma membrane into numerous coexisting domains. Nat Cell Biol 14(6):640–648. doi:10.1038/ncb2487

Spokoini R, Moldavski O, Nahmias Y, England JL, Schuldiner M, Kaganovich D (2012) Confinement to organelle-associated inclusion structures mediates asymmetric inheritance of aggregated protein in budding yeast. Cell Rep 2(4):738–747

Stagge F, Mitronova GY, Belov VN, Wurm CA, Jakobs S (2013) Snap-, CLIP- and Halo-Tag labelling of budding yeast cells. PLoS One 8(10):e78745

Swayne TC, Zhou C, Boldogh IR, Charalel JK, McFaline-Figueroa JR, Thoms S et al (2011) Role for cER and Mmr1p in anchorage of mitochondria at sites of polarized surface growth in budding yeast. Curr Biol 21(23):1994–1999

van de Linde S, Löschberger A, Klein T, Heidbreder M, Wolter S, Heilemann M et al (2011) Direct stochastic optical reconstruction microscopy with standard fluorescent probes. Nat Protoc 6(7):991–1009

Voelkel-Meiman K, Taylor L, Mukherjee P (2013) SUMO localizes to the central element of synaptonemal complex and is required for the full synapsis of meiotic chromosomes in budding yeast. PLoS Genet 9(10):e1003837. doi:10.1371/journal.pgen.1003837

Wildanger D, Medda R, Kastrup L, Hell SW (2009) A compact STED microscope providing 3D nanoscale resolution. J Microsc 236(1):35–43

Wisniewski J, Hajj B, Chen J, Mizuguchi G, Xiao H (2014) Imaging the fate of histone Cse4 reveals de novo replacement in S phase and subsequent stable residence at centromeres. ELife (Europe PMC Article—Europe PubMed Central)